

ORIGINAL ARTICLE

Clinical characteristics on low-dose high-resolution computed tomography and serum tumor markers of malignant pulmonary solid small nodules and postoperative survival analysis

Rui Fang^{1*}, Haicheng Han^{1*}, Yong Yang^{2*}, Chenyang Ma^{3*}, Baisheng Xie¹, Xiaoqing Fu², Wei Lu³, Lidan Xu¹, Dan Wang¹

¹School of Medicine, Hangzhou Normal University, Hangzhou, 310018, P.R.China; ²Guangxing Hospital Affiliated to Zhejiang Chinese Medical University, Hangzhou, 310007, P.R.China; ³The Third Clinical Medical College, Zhejiang Chinese Medical University, Hangzhou, 310053, P.R.China

*These authors contributed equally to this work.

Summary

Purpose: To observe the clinical features of low-dose, high-resolution computed tomography (LDCT) and changes in serum tumor markers in malignant pulmonary solid small nodules (MPSSN), and to analyze the difference in survival of patients with malignant and benign PSSN 3 years after surgery.

Methods: Patients were enrolled from the thoracic surgery department of three hospitals. According to pathological diagnosis, all patients were divided into the case group (MPSSN, n=157) and the control group (BPSSN, n=75). There were no significant differences in gender, smoking habit, and family disease history. All subjects were subjected to LDCT. Four serum tumor markers (CEA, SCC, NSE, ProGRP) were examined simultaneously. Two independent sample t-tests, Mann-Whitney U rank sum test and Pearson chi-square test were used for comparisons. Two-category logistic regression was performed to analyze LDCT index and serum tumor markers levels of the two groups. ROC curve was used to evaluate the diagnostic sensitivity and specificity of relevant indicators. Kaplan-Meier method, log-rank and generalized Wilcoxon test were used to analyze the survival rate of patients after surgery.

Results: In univariate analysis, age, nodule size, bronchial aeration sign, bronchial truncation sign, burr sign, smooth

sign and lobulated sign, SCC, NSE, and ProGRP were significantly different between two groups ($p < 0.05$ or 0.01). In the regression analysis, there was a significant correlation between MPSSN and age (X1) [95%CI (1.272, 5.257), $p = 0.009$], nodule size (X2) [95%CI (1.066, 2.746), $p = 0.041$], bronchial aeration sign (X3) [95%CI (1.384, 11.425), $p = 0.010$], bronchial truncation sign (X4) [95%CI (1.269, 13.444), $p = 0.018$] and burr sign (X5) [95%CI (0.054, 0.661), $p = 0.009$], ProGRP (X10) [95%CI (1.302, 2.439), $p = 0.040$]. The stepwise regression equation is $\text{Logistic}(p) = -3.014 + 0.950 X1 + 0.064 X2 + 1.380 X3 + 1.419 X4 - 1.666 X5 + 0.263 X10$. Log-rank and generalized Wilcoxon test analysis showed no difference in survival rate between the two groups (log rank $p = 0.271$, generalized Wilcoxon, $p = 0.139$).

Conclusions: The levels of CEA, SCC, NSE and ProGRP in MPSSN were increased; age, nodule size, bronchial aeration sign, bronchial truncation sign and burr sign had predictive value for MPSSN. Patients with PSSN had better survival rates at 3 years after surgery.

Key words: malignant pulmonary solid small nodules, computed tomography, high risk factors, serum tumor markers, survival, case-control study

Introduction

The mortality rate of malignancies has been increasing year by year, and it is becoming a common public health problem all over the world [1].

In the past two or three decades, lung cancer has been the most common malignancy in the world with the highest morbidity and mortality [2]. The

incidence of lung cancer is expected to significantly increase not only in developed countries, such as USA, but also in developing countries, such as China [3,4]. According to the 2015 China Cancer Statistics Report, the expected morbidity and mortality rate of lung cancer in China are both the highest [5]. According to the National Cancer Center registration data, the incidence of lung cancer in 2013 was as high as 53.86/10⁵, and the mortality rate was 43.41/10⁵ [6]. The incidence of lung cancer in recent years shows an increasing trend [7].

In recent years, with the continuous improvement of people's health awareness and the popularization of high-resolution computed tomography (CT) examination, the detection rate of small nodules in the lung is gradually increasing. Pulmonary nodules are defined as round or irregular lesions with a diameter ≤ 3 cm [8]. CT is characterized by increased density of opacities, which can be single or multiple, with clear or unclear borders. Among them, nodules ≤ 2 cm are called pulmonary small nodule. The percentage of malignant pulmonary small nodules > 1 cm in diameter is as high as 50 to 60% [9]. According to its tumor histology, lung cancer is divided by WHO into epithelial tissue origin and mesenchymal tissue origin, and the epithelial tissue origin is more common. Lung cancer of epithelial tissue origin include adenocarcinoma, squamous cell carcinoma, neuroendocrine carcinoma, large cell carcinoma, adenosquamous carcinoma, other unclassified cancers, and adenomas [10]. In the malignant pulmonary solid small nodules (MPSSN), adenocarcinoma, squamous cell carcinoma, adenosquamous carcinoma and carcinoid are more common. Early precise and simple diagnosis is the key for the diagnosis and treatment of lung cancer. At present, the 5-year survival rate of lung cancer is only 15.6%, while in patients with stage IV NSCLC is only 13% [11]. Therefore, the screening for diagnosis of early lung cancer, especially the early diagnosis and treatment of pulmonary malignant small nodules, is of great prognostic significance.

At present, low-dose spiral CT, liquid biopsy of sputum or blood, and new fiberoptic bronchoscopy techniques are mainly used for early screening of lung cancer. Serum tumor markers in liquid biopsies, such as CEA, CA125, CA15.3, Cyfra21-1 [12-14], have shown high sensitivity in the diagnosis of middle and advanced lung cancer, but their sensitivity for early diagnosis of lung cancer is not clear [15]. Currently, the detection of circulating tumor cells (CTCs), and circulating tumor nucleic acid (including circulation tumor DNA and circulating tumor RNA) in liquid biopsy has attracted considerable attention. CTCs are superior to traditional tumor markers in distinguishing benign

from malignant pulmonary nodules [16]. One study has shown that CTCs can be detected in peripheral serum in early lung cancer even before the formation of small lesions [17]. CTCs can also be used to guide clinical medication and analysis of patient prognosis [18,19]. However, the diagnostic sensitivity of CTCs is unclear.

Currently, low-dose high-resolution thin-layer CT has been widely used in early screening program for lung cancer in China, especially for pulmonary nodules with a diameter ≤ 3 cm. Proper treatment following early detection of pulmonary small nodules (including ground glass nodules (GGNs), partial solid nodules, and fully solid nodules) may improve the 5-year survival rates of patients with early-stage lung cancer. The life expectancy of these patients even exceeds 10 years [20]. However, studies have shown that there is a high trend towards malignancy in pulmonary small nodules. More than half of the small pulmonary nodules > 1 cm in diameter are prone to malignant transformation [21], non-calcified solid nodules (without typical benign nodular features), with a diameter greater > 8 mm or a volume greater > 300 mm [22]. Burrs on the boundary, are more likely to be malignant [23], and some pGGNs also have the potential for growth and malignant transformation [24,25]. In addition, there is a positive correlation between age, nodule size and MPSSN.

At present, serum tumor markers for lung cancer are mainly CEA, NSE, SCC, CYFRA21-1 and ProGRP. CEA is an acidic glycoprotein that is synthesized in the small intestine, liver, and pancreas during the embryonic period. The level of serum CEA in adults is extremely low, but it is elevated in many tumors. CEA has a high positive rate for the diagnosis of lung cancer, and has good monitoring values for tumor invasion and metastasis [15]. Its sensitivity as a marker for lung cancer is 35 to 77% [26]. NSE is present in nerve tissue and the neuroendocrine system. Small cell lung cancer (SCLC) is a neuroendocrine tumor that secretes NSE. Therefore, NSE has certain value for the diagnosis and treatment monitoring of SCLC [27]. SCC is an antigen produced and secreted by squamous cell carcinoma and is highly specific for patients with advanced lung squamous cell carcinoma. CYFRA21-1 is an acidic polypeptide mainly present in the cytoplasm of lung tumor epithelium, which can be degraded by protease or released into the blood as dissolved fragments after cell dead. Especially in the diagnosis of lung squamous cell carcinoma, CYFRA21-1 has good sensitivity and specificity and is a new tumor marker for clinical use in recent years [28]. ProGRP has high diagnostic sensitivity and specificity for SCLC and can be used as a marker for

SCLC to reflect the condition and treatment effect of SCLC [29].

However, there is still no ideal marker for early clinical diagnosis, especially the sensitivity of a single marker is not high. Blind joint detection of all tumor markers will inevitably increase the economic burden and waste medical resources. Therefore, the performances of different combinations of markers should be tested. Currently, nodular biopsy, CT guided puncture and thoracoscopic surgery are often used in the early detection of pulmonary nodules. Compared with traditional methods of diagnosis and treatment, thoracoscopic techniques have many advantages such as small trauma and quick recovery. The key for the application of thoracoscopic techniques in the diagnosis and treatment of pulmonary small nodules is the accurate localization of small nodules. The purpose of diagnosis and treatment of benign lesions can be achieved once, and for malignant lesions, radical surgery is performed to achieve early diagnosis and early treatment. However, postoperative distant recurrence may occur, which causes long-term pain or other complications. In addition, misdiagnosis also happens [20].

In this study, the clinical features of low-dose, high-resolution CT and tumor markers CEA, SCC, NSE, ProGRP, and CYFRA21-1 for malignant transformation of PSSN were analyzed. The survival rate of patients with MPSSN for 3 years was observed, and complications affecting the quality of life and causing deaths were analyzed.

Methods

Subjects and groups

Enrolled patients were from the department cardiothoracic surgery of Guangxing Hospital Affiliated to Zhejiang Chinese Medical University, the First Affiliated Hospital of Zhejiang University and Peking University People's Hospital from June 2014 to June 2017. All patients were subjected to low dose, high-resolution CT and the tumor markers CEA, SCC, NSE, ProGRP, CYFRA21-1 were examined. Patients with pathologically diagnosed MPSSN composed the case group, and patients with pathologically confirmed benign pulmonary solid small nodules (BPSSN) composed the control group.

Diagnostic criteria

Diagnosis of the case group (patients with MPSSN) was performed according to the "stage of lung cancer" in the "Guidelines for the diagnosis and treatment of primary lung cancer (2011 edition)" established by the China Society of Clinical Oncology (CSCO) Guidelines Working Committee [30]. TNM stages were determined according to the criteria established by International Association for the Study of Lung Cancer (IASLC) 2009 (7th Edn): "T1a: maximum tumor diameter ≤ 2 cm, T1b: maximum tumor diameter >2 cm and ≤ 3 cm", "N0: no regional lymph node metastasis" and "M0: no distant metastasis" [31]. The control group was diagnosed as benign pulmonary solid nodules by CT and pathology [8]. Measurement of solid ingredients was performed according to the standards established by the Fleischner Society [32]. CT features of PSSN (complete solid nodules and partial solid nodules) are shown in Figure 1.

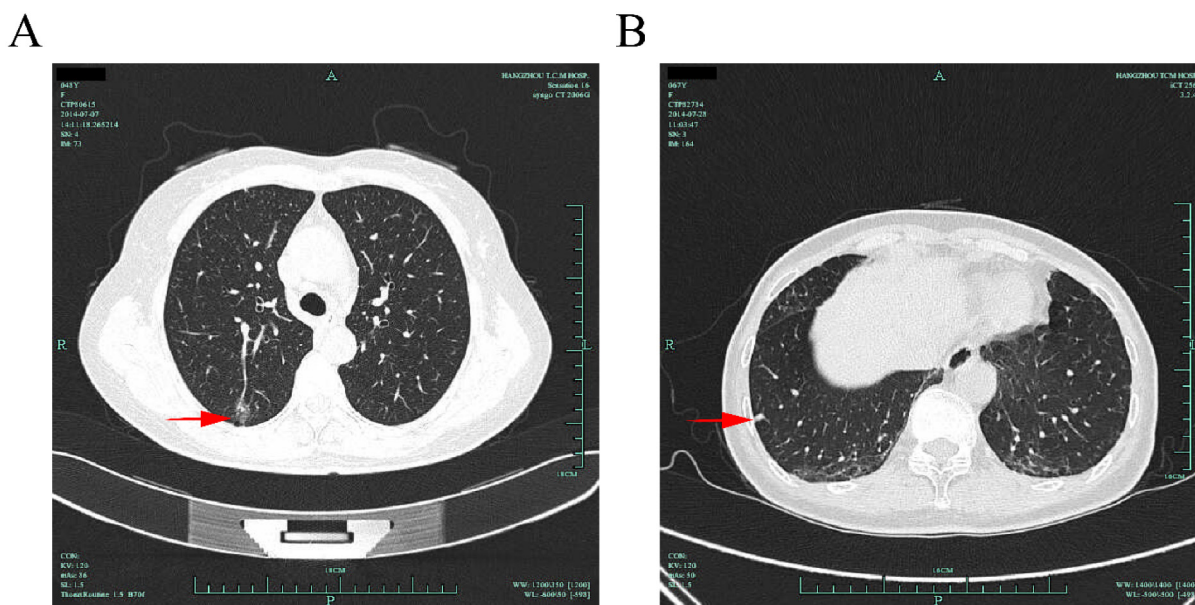


Figure 1. Low-dose CT imaging features of pulmonary solid small nodules. Typical features of common locations in MPSSN. **A:** 48-year-old woman has MPSSN. The CT image shows an elliptical shape with a well-defined heterogeneity mass (arrow) with significant partial solid enhancement. **B:** 67-year-old woman with MPSSN. The CT image shows a clearly enhanced elliptical shape with a clear solid mass (arrow).

Inclusion and exclusion criteria

Age >18 years and <80 years, Karnofsky performance status (PS) score>80, and patients volunteered to participate in the study and could cooperate with the researchers. Patients with pathological diagnosis as MPSSN were excluded in the control group. Patients with ground-glass nodules and history of previous malignancy were excluded from both groups. Patients underwent tumor-related treatment, and those with a history of lobectomy or pneumonectomy were excluded. Patients with serious infection, severe heart disease and stent placement, serious primary diseases such as liver and kidney, hematopoietic system, nervous system, mental illness and pregnant women were excluded.

Ethical review

This project passed the ethical review of the Ethics Committee of Guangxing Hospital Affiliated to Zhejiang Chinese Medical University (Examination Approval No. 2014 LL001).

Information extraction and specimen collection

General data were answered by the respondents, such as gender, age, ethnicity, marital status, educational level and dietary habits, smoking and drinking habits, exercise habits, and past history and family history of other cancer. All patients were subjected to low-dose, high-resolution (512*512 matrix) 128-row 256i CT examinations. Four mL fasting venous blood were taken from each patient. The blood was naturally agglutinated for 30 min, and then was centrifuged at 2300 g for 8 min at 8 °C to separate serum. Serum was stored at -80 °C until use.

Detection reagents and instruments

Philips 128 row 256iCT. CEA, NSE kit and DiaSorin-XL Chemiluminescence Immunoassay (DiaSorin, Italy).

SCC, ProGRP kit and i2000SR chemiluminescence immunoassay analyzer (Abbott, USA).

Specimen detection and quality control

The 128-row 256iCT line was tested by low-dose FBP/IR method. The other parameters were: tube voltage 120 Kvp, collimation 128×0.625 mm, pitch 0.915, 0.5 s/Rot, layer thickness 5 mm, FOV 300-330 mm; the layer thickness of scanning was 5 mm, the reconstruction layer was 1.5 mm thick, and the 512*512 matrix was reconstructed. Enhanced CT examination was performed in partial solid nodules.

Concentrations of CEA and NSE were measured by DiaSorin-XL automatic chemiluminescence immunoassay analyzer. Values of NSE, SCC and ProGRP were detected by i2000SR chemiluminescence immunoassay analyzer.

Establishing database

A database was established, including patient general information (gender, age, ethnicity, marital status, educational level, etc), smoking and drinking preference, past history and family history of other cancer, CT findings (nodule type, the nodule site, nodule size and lesion signs), and 4 serum lung cancer markers (CEA, SCC, NSE, ProGRP).

Data processing and statistical analysis

The missing data were filled by the Multiple Imputation (MI) and Mean/Mode Completer methods of the SAS 13.0 software. Data were analyzed by SPSS version 23.0 for Windows (SPSS Inc, Chicago, IL, USA). Chi square test and t-test were used to determine the consistency of baseline data between the two groups. The continuous variables were compared using pairwise analysis. The Dunnett method was used when the variance was homogeneous, and the Mann Whitney U test

Table 1. Baseline data analysis of two groups of patients

Variables	Categorical variables	Cases	Case group (n=157)	Control group (n=75)	χ^2	p value
Sex	Male	101	65	36	0.899	0.396
	Female	131	92	39		
Age, years	<60	136	77	59	18.360	0.000
	≥60	96	80	16		
Ethnicity	Han nationality	215	145	70	0.071	0.521
	Minority	17	12	5		
Marriage status	Married	208	140	68	0.006	0.571
	Unmarried and divorced	22	15	7		
Education	Junior high school and below	115	77	28	5.87	0.053
	High school, technical secondary	76	45	31		
	College and above	51	35	26		
Smoking	Yes	66	48	18	1.077	0.189
	No	166	109	57		
Family history of cancer	Yes	36	22	14	0.920	0.220
	No	196	135	61		

was used when the variance was not uniform. Count data were subjected to χ^2 test or the rank sum test. Multivariate correlation analysis was performed using logistic regression analysis, and correlation heat maps between indicators were drawn using R software. Continuous variables with normal distribution were presented as mean \pm standard deviation (SD), non-normal variables were reported as median, $p < 0.05$ was considered statistically significant. Reactive oxygen species (ROC) curve was used to analyze the diagnostic sensitivity and specificity of low-dose computed tomography and tumor markers for MPSSN based on the cut off value. Sensitivity=true positive number / (true positive number + false negative number) \times 100%; specificity=true negative number / (true negative number + false positive number) \times 100%. Kaplan-Meier method was used to plot survival curves, and the log rank test and the generalized Wilcoxon test were used to compare survival curves.

Results

General information

There were 65 males and 92 females in the case group, and 36 males and 39 females in the control group. After the χ^2 test, gender, ethnicity, marital status, education level, smoking history, and family history of cancer were balanced in the case and the control group. The p values were 0.396, 0.521, 0.571, 0.053, 0.189 and 0.220, respectively. There were significant differences in age between the two groups ($p=0.000$), as shown in Table 1. In addition, the average nodule size of the patients in the case group was 13.649 ± 4.481 mm, while the average nodule size of the control group was 11.266 ± 5.129 mm ($p=0.043$). In the case group, adenocarcinoma,

squamous cell carcinoma, large cell carcinoma, small cell carcinoma, and carcinoid were 59, 27, 15, 18 and 11 cases, respectively. Most cases in the control group were hamartomas and chondromas. There were 84 cases of complete solid nodules and 73 cases of partial solid nodules in the case group, while there were 32 cases of complete solid nodules and 43 cases of partial solid nodules in the control group.

Univariate analysis of LDCT and tumor markers in the two groups of patients

To compare age, CT features and serum tumor markers between the two groups of patients, two independent sample t -tests (age, nodule size), Mann-Whitney U rank sum test (CEA, SCC, NSE, ProGRP) and Pearson χ^2 test (nodular site, vacuole sign, bronchial aeration sign, bronchial truncation signs, burr signs, smooth signs, lobulated signs, pleural indentation signs, vascular bundle signs) were performed. The results showed that CEA (Z value=-1.788, $p=0.074$), nodule site ($\chi^2=2.543$, $p=0.074$), vacuole sign ($\chi^2=1.046$, $p=0.306$), pleural indentation sign ($\chi^2=2.692$, $p=0.101$) and vascular bundle sign ($\chi^2=0.449$, $p=0.503$) were not significantly different between the two groups of patients. Age, nodule size, bronchial aeration sign, bronchial truncation sign, burr sign, smooth sign and lobulated sign, SCC, NSE, ProGRP were statistically different between the two groups of patients (Table 2). Among them, SCC was increased significantly in squamous cell lung carcinoma, while NSE and ProGRP increased significantly in small cell lung cancer.

Table 2. Comparison of low-dose computed tomography and tumor markers in the two groups of patients

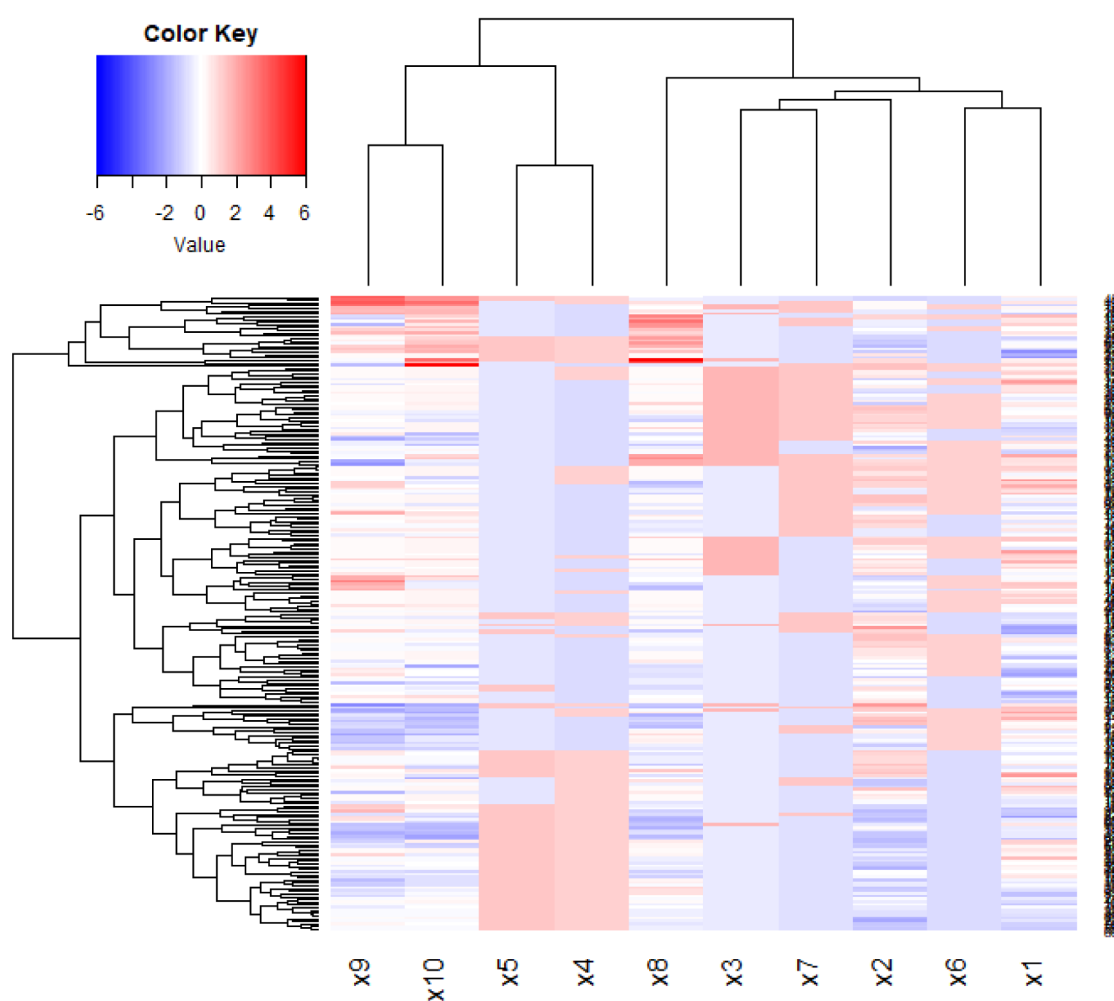
	Age (years)	Nodule size (mm)	SCC (mg/L)	NSE (ng/ML)	ProGRP (PG/mL)					
Case group	58.847±10.883	13.649±4.481	0.936±0.429	12.388±4.203	2.714±1.005					
Control group	54.546±9.294	11.266±5.129	0.784±0.372	11.798±4.149	2.369±0.889					
F/Z value	4.674	4.160	-3.830	-2.789	-3.381					
P value	0.032	0.043	0.000	0.005	0.001					
Two independent sample t-tests and Man-Whitney U rank sum test										
	Bronchial aeration sign		Bronchial truncation sign		Burr sign		Smooth sign		Leaf sign	
	(-)	(+)	(-)	(+)	(-)	(+)	(-)	(+)	(-)	(+)
Case group	104	53	94	63	123	34	74	83	92	65
Control group	70	5	34	41	32	43	55	20	60	15
x²	19.876	4.338	29.135	14.113	10.290					
p	0.000	0.037	0.000	0.000	0.001					

Pearson chi-square test was used

Table 3. Logistic regression analysis of low-dose computed tomography and tumor markers of MPSSN

Variables	B	S.E	Wald		Odd ratio (95%CI)	p value
Age (X1)	0.95	0.362	6.885		2.586 (1.272-5.257)	0.009
Nodule size (X2)	0.064	0.037	3.035		1.992 (1.066-2.746)	0.041
Bronchial aeration sign (X3)	1.38	0.538	6.573		3.977 (1.384-11.425)	0.01
Bronchial truncation sign (X4)	1.419	0.602	5.552		4.131 (1.269-13.444)	0.018
Burr sign (X5)	-1.666	0.639	6.805		0.189 (0.054-0.661)	0.009
Smooth sign (X6)	0.496	0.477	1.084		1.642 (0.645-4.179)	0.298
Leaf sign (X7)	0.133	0.422	0.1		1.143 (0.500-2.612)	0.752
SCC (X8)	0.331	0.639	0.268		1.392 (0.398-4.872)	0.605
NCE (X9)	0.021	0.061	0.119		1.021 (0.906-1.151)	0.73
ProGRP (X10)	0.263	0.341	0.596		1.695 (1.302-2.439)	0.04
constant	-3.014	1.072	7.901		0.049	0.005

Two-class Logistic was used

**Figure 2.** Interactive heat map of low-dose computed tomography and tumor markers of MPSSN. The Figure shows a heat map of the selected tumor markers features. Each row of the heat map represents a tumor marker feature, with each column representing the patient. From the heat map, we can directly observe the distribution characteristics of the tumor marker features Z-Score in the dataset: there are differences in the Z scores of similar tumor marker features, and patients with certain specific markers are more sensitive.

Logistic regression analysis of MPSSN based on LDCT and tumor markers

Two-class logistic regression analysis was performed with benign and malignant PSSN as dependent variables, and age, nodule size, bronchial aeration sign, bronchial truncation sign, burr sign, smooth sign and lobulated sign, SCC, NSE and ProGRP as independent variables. The logistic model using stepwise regression method was statistically significant ($\chi^2=64.562$, $p=0.000$). The model correctly explained 75.0% of the subjects. MPSSN had certain correlations with age (X1) [95%CI (1.272, 5.257), $p=0.009$], nodule size (x^2) [95% CI (1.066, 2.746), $p=0.041$], bronchus inflatable sign (X3) [95% CI (1.384, 11.425), $p=0.010$], bronchial truncation sign (X4) [95% CI (1.269, 13.444), $p=0.018$] and burr sign (X5) [95% CI (0.054, 0.661), $p=0.009$], ProGRP (X10) [95% CI (1.302, 2.439), $p=0.040$]. Simultaneously, there was a certain intrinsic correlation between the indicators of CT and tumor markers (Table 3,

Figure 2), and the stepwise regression equation is $\text{Logistic}(p)=-3.014+0.950 X1+0.064 x^2+1.380 X3+1.419 X4-1.666 X5+0.263 X10$.

Reliability and validity test of diagnostic model variables

The area under the ROC curve of age (X1), nodule size (x^2), bronchial aeration sign (X3), bronchial truncation sign (X4) and burr sign (X5), and ProGRP (X10) were 0.648 (0.575-0.722), 0.638 (0.557-0.719), 0.635 (0.564-0.707), 0.573 (0.494-0.652), 0.678 (0.602-0.755) and 0.636 (0.558-0.714), respectively. Sensitivity and specificity of age (X1), nodule size (x^2), bronchial aeration sign (X3), bronchial truncation (X4), burr sign (X5) and ProGRP (X10) for the diagnosis of MPSSN were 51.0% and 78.66%, 83.4% and 45.33%, 33.8% and 93.33%, 54.7% and 59.87%, 57.3% and 78.34% and 60.5% and 81.33%, respectively (Table 4 and Figure 3).

Table 4. Sensitivity and specificity of diagnostic model for MPSSN

Test result Variables	Area Under the Curve	Std. error ^a	Asymptotic Sig ^b	95% Confidence interval	Sensitivity	Specificity	Youden index
Age (X1)	0.648	0.038	0.000	0.575-0.722	0.510	0.786	0.296
Nodule size (X2)	0.638	0.041	0.001	0.557-0.719	0.834	0.453	0.287
Bronchial aeration sign (X3)	0.635	0.037	0.001	0.564-0.707	0.338	0.933	0.271
Bronchial truncation sign (X4)	0.573	0.040	0.073	0.494-0.652	0.547	0.599	0.145
Burr sign (X5)	0.678	0.039	0.000	0.602-0.755	0.573	0.783	0.356
ProGRP (X10)	0.636	0.040	0.001	0.558-0.714	0.605	0.813	0.418

The test result variables: predicted probability, predicted ^a under the nonparamant assumption, ^bnull hypothesis:true area=0.5

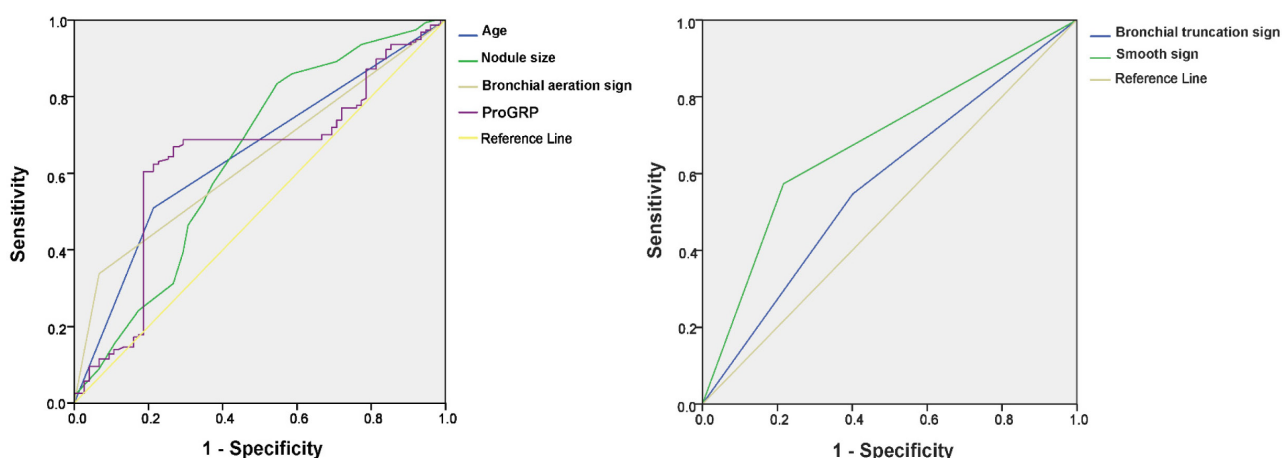


Figure 3. ROC curve of low-dose computed tomography and tumor markers in the diagnostic model for MPSSN. The area under the ROC curve of tumor markers [age (X1), nodule size (X2), bronchial aeration sign (X3), bronchial truncation sign (X4) and burr sign (X5), and ProGRP (X10)] were 0.648 (0.575-0.722), 0.638 (0.557-0.719), 0.635 (0.564-0.707), 0.573 (0.494-0.652), 0.678 (0.602-0.755) and 0.636 (0.558-0.714).

Survival analysis after operation in both groups

Eighty-nine out of 157 patients with MPSSN completed 3-year follow-up. Among them, 4 patients died, and the survival rate was 95.51%. Of the 4 deaths, 2 patients died of lung cancer and 2 died of heart disease and respiratory failure. Eighty-five patients with MPSSN survived, including 4 cases of AIS, 34 cases of invasive adenocarcinoma, and 6 cases of MIA. CT features of 68 cases were normal. There were 3 cases of small nodules in lung tissue and mediastinum, and 24 cases of dyspnea, 22 cases of cough, 19 cases of chest pain, and 12 cases of daily activities. Seventy-five patients with MPSSN were followed up for 3 years after surgery, and 59 had valid data. Three of them died, and the survival rate was 94.92%. Causes of death were heart failure, lung failure, and 1 case had malignant transformation. The remaining patients showed 7 cases of normal CT, 7 cases of dyspnea, 3 cases of cough and 6 cases of chest tightness and chest pain. The median survival of the benign and malignant patients was 32 and 37 months, respectively; the survival curve (log rank $p=0.271$, generalized Wilcoxon $p=0.139$) showed no difference in survival between the 2 groups (Figure 4).

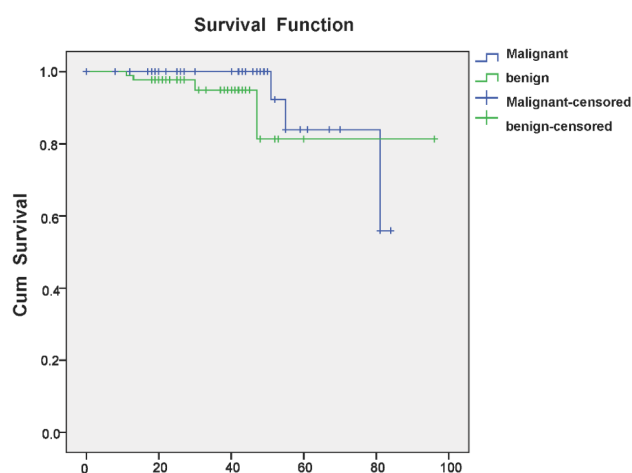


Figure 4. Kaplan-Meier survival curves of the two groups of patients after surgery (Log Rank $P=0.271$, Generalized-Wilcoxon $p=0.139$).

Discussion

Early lung cancer often has no typical symptoms. Its imaging feature is the existence of pulmonary nodules (high-density shadows of circular or irregular shapes with a diameter of less than 30 mm in the lung field on CT or chest radiograph, with clear or unclear boundaries) [33]. LDCT can reduce lung cancer mortality by nearly 20% [34].

With the development of imaging technology, low-dose, high-resolution CT examination has gradually become the main means of early lung cancer screening. According to the corresponding large-scale clinical research, various countries and regions around the world have established their own screening guidelines, such as the National Comprehensive Cancer Network (NCCN), American College of Chest Physicians (ACCP) [35,36], the guidelines for the assessment of Asian patients with pulmonary nodules [37], and Guidelines for the Classification, Diagnosis and Treatment of Pulmonary Nodules in China (2016 Edition) [8]. These guidelines emphasize the screening of CT features of MPSN and the patient's own risk factors.

According to its internal density, pulmonary nodules are simply divided into solid nodules, partial solid nodules and ground-glass nodules 3 types. Solid nodules are all nodules with soft tissue density inside, and the density is relatively homogeneous. Partial solid nodules refer to nodules containing both ground glass density and solid soft tissue density, and the density is not homogeneous [33]. As a non-specific CT manifestation, ground glass-like nodules can be caused by a variety of lesions including inflammation and atypical adenomatoid hyperplasia. However, partial solid nodules containing ground glass density have a higher probability of malignancy. This is consistent with the various guidelines, that partial solid nodules have the highest degree of malignancy, followed by purely ground glass density nodules and solid nodules.

For partial solid nodules with the highest degree of malignancy, some studies suggest that the larger the diameter of the actual part, the higher the degree of malignancy. The part of the micro-invasive adenocarcinoma is partial solid nodules, and a few of them appear as solid nodules. If the partial solid diameter of the invasive lung cancer is greater than 5 mm, or the total area (consolidation-to-tumor ratio) is larger than 25%, or the tumor mediastinal window disappearance rate (tumor disappearance ratio) is less than 50%, it often suggests that the nodules have developed infiltration. For partial solid nodules, it can be seen that the larger the diameter of the actual part of the partial solid nodules, the more the chance of malignancy [22]. The size of pulmonary nodules is highly correlated with their pathological properties. Some studies have even concluded that the diameter is an independent risk factor for benign and malignant judgments, while the diameter of benign nodules is relatively small. This study also draws similar conclusions. The occurrence of lung cancer undergoes a series of stages such as hyperplasia - atypical hyperplasia - carcinoma in situ - invasive cancer, etc,

which is a process in which the tumor gradually enlarges [38]. This study shows that the size of pulmonary nodules is closely related to the degree of malignancy, and the larger the nodules, the higher the degree of malignancy. It was also found that when pulmonary nodules were ≥ 14 mm in size, the levels of tumor markers were significantly elevated, and LDCT was performed 3 months after screening. If a pulmonary nodule is enlarged, it is necessary to have a consultation with a senior doctor to decide whether to enter clinical treatment [39].

The characteristics of a pulmonary nodule itself are also an important basis for judging its pathological benign or malignant nature. The bronchial aeration sign is due to the adherent growth of tumor cells, and the alveolar bronchioles that have not destroyed in the lesion are still preserved, and the tumor cells and peripheral fibrous tissue proliferate and lead to bronchiectasis [40]. Bronchial inflatable signs are common in malignant tumors, and benign tumors can also be seen [41]. Bronchial truncation is mainly caused by tumor cells growing along the bronchial wall or compressing the adjacent bronchi to cause bronchial stenosis or truncation. It mainly occurs in central lung cancer, less in SPN [42]. The burr sign is the result of tumor tissue infiltrating into adjacent bronchi, vascular sheath or regional lymph nodes, or tumor connective tissue hyperplasia. The burr sign is also one of the characteristics of malignant pulmonary nodules, while smooth sign is a possible protective factor for pulmonary connective tissue, which is consistent with previous reports in China [43]. This study also showed that the bronchial aeration sign and burr sign of pulmonary nodules closely correlated to their pathological properties.

Detection of serum tumor markers plays an important role in the diagnosis of lung cancer. However, due to the lack of sufficient sensitivity and specificity in the diagnosis of lung cancer by a single marker, multiple tumor markers are often used in combined diagnosis. The levels of serum CEA, NSE, CYFRA21-1 and ProGRP not only contribute to the early diagnosis of lung cancer patients, but also help to judge the prognosis of lung cancer [44-46]. This article also monitored serum CEA, NSE, SCC and ProGRP levels in benign and malignant PSSN, and the results of this study indicate that although the levels of tumor markers in MPSSN patients are indeed higher than those in BPSSN patients, the sensitivity to lung cancer diagnosis is relatively low. After the variable selection of logistic regression analysis, after introducing CEA, NSE, SCC and ProGRP variables in turn, the sensitivity, specificity and Youden index of computed tomography detection combined

with ProGRP to the diagnosis of lung cancer were 60.5% and 81.33% respectively, and the sensitivity and the Youden index was larger than those of the individual markers. Because of the close relationship between tumor markers and TNM staging of lung cancer, MPSSN (diameter less than 2 cm) is stage I lung cancer in this study. Although serum tumor markers were elevated, their contribution in early diagnosis was not significant. The elevation of ProGRP may be caused by interactions between variables. It indicated that in the early stages of malignancy, when CT examination has not yet been positive, the elevation of serum tumor markers has certain enlightenment value for tumor diagnosis, histological classification, clinical stage, prognosis and efficacy monitoring [47].

A number of studies have confirmed that CT-guided biopsy has a diagnostic accuracy of more than 90% for pulmonary nodules. Surgery is considered the preferred treatment for clinically curing lung cancer patients [48,49]. At present, with the stricter control of tobacco, the incidence of squamous cell carcinoma reduced significantly, and the incidence of lung adenocarcinoma is relatively increased. Pulmonary adenocarcinoma is usually prone to early blood metastasis, so early surgery is more important. In this study, all patients with MPSSN were treated with thoracoscopic surgery, and their 3-year survival rate was not different from BPSSN. The 5-year survival rate was only about 50%. Although there were still different degrees of complications in the two groups, the survival time after surgery increased. It also suggests that there is still room for improvement in the postoperative follow-up and treatment.

Based on the patient's own risk factors combined with the CT of PSSN and the characteristics of tumor markers, we determined the incidence of MPSSN to a certain extent in this study. The patients who were observed to find pulmonary small nodules by physical examination embodies the concept of "early detection, early diagnosis and early treatment" for malignant diseases. The results show that the size of pulmonary nodules closely related to MPSSN and the possibility of malignancy increases with the increase of pulmonary nodules. For smaller pulmonary nodules, they also required to follow-up with their own risk factors. The nature of pulmonary nodules also correlates with the degree of malignancy, and partial solid nodules have the highest degree of malignancy. The characteristics of pulmonary nodules, such as bronchial aeration and burr signs, are typical manifestations of early lung adenocarcinoma imaging. After 3 years of follow-up, the survival time of patients with pulmonary nodules was improved. However, because

the sample size is relatively small and the TNM staging is not clear, there are some limitations in this study, and the results need to be further verified by a large prospective cohort study. At the same time, with the help of CT technology, pathological diagnosis, tumor marker detection, molecular biology technology and large data technology, more risk factors for early MPSSN may be found from the microscopic point of view. More mature and sensitive lung cancer joint prediction model is established, so as to improve screening effectiveness and better guide the early stage of lung cancer clinical evaluation and post-hospital rehabilitation.

Acknowledgments

This work was supported by the Science and Technology Project of Zhejiang Province (Major Science and Technology Program) (No.2013C030443), and the Agricultural and Social Development Scientific Research Program of Hangzhou (No. 20180417A03).

Conflict of interests

The authors declare no conflict of interests.

References

1. Torre LA, Siegel RL, Ward EM, Jemal A. Global cancer incidence and mortality rates and trends - an update. *Cancer Epidemiol Biomarkers Prev* 2016;25:16-27.
2. Ferlay J, Soerjomataram I, Dikshit R et al. Cancer incidence and mortality worldwide: sources, methods and major patterns in GLOBOCAN 2012. *Int J Cancer* 2015;136:E359-86.
3. Siegel RL, Miller KD, Jemal A. Cancer Statistics, 2017. *CA Cancer J Clin* 2017; 67:1-24.
4. Fei WU, Lin GZ, Zhang JX. An Overview of Cancer Incidence and Trend in China. *Chin Cancer* 2012;21:81-5.
5. Chen W, Zheng R, Baade PD et al. Cancer statistics in China, 2015. *CA Cancer J Clin* 2016;66:115-32.
6. Chen W, Zheng R, Zhang S, Zeng H, Zou X, Hao J. Report of Cancer Incidence and Mortality in China, 2013. *Chin Cancer* 2017;26:1-7.
7. Torre LA, Bray F, Siegel RL, Jacques F, Joannie LT, Ahmedin J. Global cancer statistics, 2012. *CA Cancer J Clin* 2015;65:87-108.
8. Zhou Q, Fan Y, Wang Y et al. China National Guideline of Classification, Diagnosis and Treatment for Lung Nodules (2016 Version). *Zhongguo Fei Ai Za Zhi* 2016;19:793-8.
9. Su TH, Fan YF, Jin L, He W, Hu LB. CT-guided localization of small pulmonary nodules using adjacent microcoil implantation prior to video-assisted thoracoscopic surgical resection. *Eur Radiol* 2015;25:2627-33.
10. Yang X, Lin D. Changes of 2015 WHO Histological Classification of Lung Cancer and the Clinical Significance. *Zhongguo Fei Ai Za Zhi* 2016;19:332-6.
11. Woodard GA, Jones KD, Jablons DM. Lung Cancer Staging and Prognosis. *Cancer Treat Res* 2016;170:47-69.
12. Lee JH, Chang JH. Diagnostic utility of serum and pleural fluid carcinoembryonic antigen, neuron-specific enolase, and cytokeratin 19 fragments in patients with effusions from primary lung cancer. *Chest* 2005;128:2298-2303.
13. Okamura K, Takayama K, Izumi M, Harada T, Furuyama K, Nakanishi Y. Diagnostic value of CEA and CYFRA 21-1 tumor markers in primary lung cancer. *Lung Cancer* 2013;80:45-9.
14. Kimura Y, Fujii T, Hamamoto K, Miyagawa N, Kataoka M, Iio A. Serum CA125 level is a good prognostic indicator in lung cancer. *Br J Cancer* 1990;62:676-8.
15. Grunnet M, Sorensen JB. Carcinoembryonic antigen (CEA) as tumor marker in lung cancer. *Lung Cancer* 2012;76:138.
16. Chen YY, Xu GB. Effect of circulating tumor cells combined with negative enrichment and CD45-FISH identification in diagnosis, therapy monitoring and prognosis of primary lung cancer. *Med Oncol* 2015;32:190-7.
17. Ilie M, Hofman V, Long-Mira E et al. "Sentinel" circulating tumor cells allow early diagnosis of lung cancer in patients with chronic obstructive pulmonary disease. *PLoS One* 2014;9:e111597.
18. Gorges TM, Penkalla N, Schalk T et al. Enumeration and Molecular Characterization of Tumor Cells in Lung Cancer Patients Using a Novel In Vivo Device for Capturing Circulating Tumor Cells. *Clin Cancer Res* 2016;22:2197-2206.
19. Chen X, Wang X, He H, Liu Z, Hu J, Wei L. Combination of Circulating Tumor Cells with Serum Carcinoembryonic Antigen Enhances Clinical Prediction of Non-Small Cell Lung Cancer. *PLoS One* 2015;10:e0126276.
20. Jiang G, Chen C, Zhu Y et al. [Shanghai Pulmonary Hospital Experts Consensus on the Management of Ground-Glass Nodules Suspected as Lung Adenocarcinoma (Version 1)]. *Zhongguo Fei Ai Za Zhi* 2018;21:147-159.
21. Kha LC, Hanneman K, Donahue L et al. Safety and Efficacy of Modified Preoperative Lung Nodule Microcoil Localization Without Pleural Marking: A Pilot Study. *J Thorac Imag* 2016;31:15-22.
22. Suzuki K, Koike T, Asakawa T et al. A prospective radiological study of thin-section computed tomography to predict pathological noninvasiveness in peripheral clinical Ia lung cancer (Japan Clinical Oncology Group 0201). *J Thorac Oncol* 2011;6:751-6.

23. Callister ME, Baldwin DR, Akram AR et al. British Thoracic Society guidelines for the investigation and management of pulmonary nodules. *Thorax* 2015;70:ii1-ii54.
24. Cho S, Yang H, Kim K, Jheon S. Pathology and prognosis of persistent stable pure ground-glass opacity nodules after surgical resection. *Ann Thorac Surg* 2013;96:1190-5.
25. Eguchi T, Kondo R, Kawakami S et al. Computed tomography attenuation predicts the growth of pure ground-glass nodules. *Lung Cancer* 2014;84:242-7.
26. Wu G, Ba J, Wang E, Teng Y, Fan X. Diagnostic value of determination of CEA, CA125, CA153 and CA199 assay in pleural fluid for lung cancer. *Zhongguo Fei Ai Za Zhi* 2004;7:35-7.
27. Tiseo M, Ardizzoni A, Cafferata MA et al. Predictive and prognostic significance of neuron-specific enolase (NSE) in non-small cell lung cancer. *Anticancer Res* 2008;28:507-13.
28. Wang J, Zhang N, Li B et al. Decline of serum CYFRA21-1 during chemoradiotherapy of NSCLC: a probable predictive factor for tumor response. *Tumour Biol* 2011;32:689-95.
29. Molina R, Augé JM, Bosch X et al. Usefulness of serum tumor markers, including progastrin-releasing peptide, in patients with lung cancer: correlation with histology. *Tumour Biol* 2009;30:121-9.
30. Zhi X, Wu Y, Ma S et al. Chinese Guidelines on the Diagnosis and Treatment of Primary Lung Cancer (2011 Version). *Chin J Lung Cancer* 2012;15:677-88.
31. Vallières E, Shepherd FA, Crowley J et al. The IASLC lung cancer staging project: proposals regarding the relevance of tnm in the pathologic staging of small cell lung cancer in the forthcoming (seventh) edition of the TNM classification for lung cancer. *J Thorac Oncol* 2009;4:1049-59.
32. Naidich DP, Bankier AA, MacMahon H et al. Recommendations for the management of subsolid pulmonary nodules detected at CT: A statement from the Fleischner Society. *Radiology* 2013;266:304-17.
33. Hansell DM, Bankier AA, MacMahon H, McLoud TC, Müller NL, Remy J. Fleischner Society: Glossary of Terms for Thoracic Imaging. *Radiology* 2008;246:697-722.
34. National Lung Screening Trial Research Team, Aberle DR, Adams AM, Berg CD et al. National Lung Screening Trial Research Team. Reduced lung-cancer mortality with low dose computed tomographic screening. *N Engl J Med* 2011;365:395-409.
35. National Comprehensive Cancer Network: NCCN clinical practice guidelines in oncology: lung cancer screening v2. 2018. Washington: National Comprehensive Cancer Network. [cited 2018 Jan 02].
36. Gould MK, Donington J, Lynch WR et al. Evaluation of individuals with pulmonary nodules: when is it lung cancer? *Chest* 2013;143:93S-120S.
37. Kim YK, Lee SH, Seo JH, Kim JH, Kim SD, Kim GK. A comprehensive model of factors affecting adoption of clinical practice guidelines in Korea. *J Korean Med Sci* 2010;25:1568-73.
38. Aoki T, Nakata H, Watanabe H et al. Evolution of peripheral lung adenocarcinomas: CT findings correlated with histology and tumor doubling time. *AJR Am J Roentgenol* 2000;174:763-8.
39. Zhou Q, Fan Y, Wang Y et al. China National Lung Cancer Screening Guideline with Low-dose Computed Tomography (2018 version). *Zhongguo Fei Ai Za Zhi* 2018;21:67-75.
40. Haro A, Yano T, Kohno M, Yoshida T, Okamoto T, Maehara Y. Ground-glass opacity lesions on computed tomography during postoperative surveillance for primary non-small cell lung cancer. *Lung Cancer* 2012;76:56-60.
41. Oda S, Awai K, Murao K et al. Computer-aided volumetry of pulmonary nodules exhibiting ground-glass opacity at MDCT. *AJR Am J Roentgenol* 2010;194:398.
42. Walker ED, Brammer A, Cherniack MG, Laden F, Cavalieri JM. Cardiovascular and stress responses to short-term noise exposures-A panel study in healthy males. *Environ Res* 2016; 150:391-7.
43. Li Y, Chen KZ, Wang J. Development and validation of a clinical prediction model to estimate the probability of malignancy in solitary pulmonary nodules in Chinese people. *Clin Lung Cancer* 2011;12:313-9.
44. Zaleska M, Szturmowicz M, Zych J et al. Elevated serum NSE level in locally advanced and metastatic NSCLC predispose to better response to chemotherapy but worse survival. *Pneumonol Alergol Pol* 2010;78:14-20.
45. Holdenrieder S, von Pawel J, Dankelmann E et al. Nucleosomes, ProGRP, NSE, CYFRA 21-1, and CEA in monitoring first-Line chemotherapy of small cell lung cancer. *Clin Cancer Res* 2008;14:7813-21.
46. Tas F, Bilgin E, Tastekin D, Erturk K, Duranyildiz D. Clinical significance of serum laminin levels in patients with lung cancer. *Biomed Rep* 2016;4:485-8.
47. Hao SH, Hao L, Yang WH, Wang WG, Suo RX. The Diagnostic Value of Serum CEA, CA19-9, SCC-Ag, NSE, CYFRA21-1 and ProGRP in Lung Cancer. *Chin Cancer* 2012;21:852-855.
48. Bai C, Choi CM, Chu CM et al. Evaluation of pulmonary nodules: clinical practice consensus guidelines for Asia. *Chest* 2016;150:877-93.
49. Lee SM, Park CM, Lee KH, Bahn YE, Kim JI, Goo JM. C-arm cone-beam CT-guided percutaneous transthoracic needle biopsy of lung nodules: clinical experience in 1108 patients. *Radiology* 2014;271:291-300.